VNU Journal of Science: Medical and Pharmaceutical Sciences

Journal homepage: https://js.vnu.edu.vn/MPS

Original Article

Optimization of Self-nanoemulsifying Drug Delivery Systems Containing Andrographolide: Design of Experiment Approach

Nguyen Tran Mai Phuong, Duong Thanh Tung, Nguyen Thach Lien, Nguyen Hoang Anh, Nguyen Nhat Trang, Nguyen Thach Tung*

Hanoi University of Pharmacy, 13-15 Le Thanh Tong, Cua Nam, Hanoi, Vietnam

Received 4th February 2026
Revised 4th April 2026; Accepted 27th May 2026

Abstract: The objectives of this study were to optimize an andrographolide-loaded self-nanoemulsifying drug delivery system (SNEDDS) using a design of experiments (DoE) approach. Preformulation studies demonstrated that andrographolide exhibits low solubility and poor dissolution behavior, which may compromise its therapeutic efficacy. In parallel, molecular docking studies were conducted to explore the potential molecular mechanism of andrographolide in RCC. The results suggested that andrographolide is capable of forming favorable interactions within the active sites of VEGFR1 and VEGFR2, providing preliminary insight into its possible involvement in VEGF-related signaling pathways. A central composite design was employed to investigate the effects of formulation variables, including the oil fraction and the surfactant fraction in S_{mix}. Following optimization, the optimal formulation was obtained at an oil fraction of 0.10 and a surfactant fraction in S_{mix} of 0.61. The optimized SNEDDS exhibited a mean droplet size of 12.02 ± 0.25 nm, a polydispersity index of 0.113 ± 0.017, and good thermodynamic stability after heating-cooling cycles. The SNEDDS formulation significantly improved the dissolution behavior of andrographolide compared to the raw material, indicating its potential to overcome dissolution-limited absorption. Overall, this study demonstrates that DoE-guided optimization of an andrographolide-loaded SNEDDS, supported by preformulation insights, represents a rational and effective strategy to enhance drug dissolution and improve its pharmaceutical performance.

Keywords: Andrographolide; Design of experiments; Central composite design; SNEDDS; Lipid-based delivery.

* Corresponding author.
E-mail address: nguyenthachtung@hup.edu.vn

https://doi.org/10.25073/2588-1132/vnumps.4909

1. Introduction

Andrographolide, the major bioactive constituent of *Andrographis paniculata* (Wall. Ex Nees), is a promising compound that has demonstrated encouraging anticancer activity in several types of cancer, including lung, breast, colorectal, with particular relevance to renal cell carcinoma (RCC) [1-5]. However, like many other natural compounds, the clinical application of andrographolide is limited by its poor solubility, low dissolution rate, and inadequate permeability [6]. In recent years, lipid-based drug delivery systems have attracted considerable attention in pharmaceutical formulation due to their notable advantages in enhancing bioavailability and improving drug stability. Among lipid-based formulations, self-emulsifying drug delivery systems (SEDDS) represent a promising technology for enhancing both the rate and extent of absorption of poorly water-soluble drugs [7]. In cancer therapy, SEDDS exhibit several advantageous properties, including prolonged circulation time, high drug-loading capacity, and the ability to encapsulate both hydrophilic and lipophilic compounds. These features make SEDDS particularly suitable for stabilizing labile therapeutics such as biologics (e.g., siRNA, DNA, and peptides) [8, 9]. Notably, SEDDS have shown potential to improve therapeutic efficacy in difficult-to-treat cancers by enhancing cellular uptake while simultaneously reducing systemic toxicity [10, 11].

In preliminary screening studies, andrographolide was formulated as SNEDDS using Labrafil M 1944 CS, Tween 80, and Transcutol HP, yielding a droplet size of 145.5 ± 2.7 nm. The ADG-loaded SNEDDS significantly reduced cell viability to 74.2% at 200 µM in Renca cells, whereas andrographolide formulated as polymeric micelles or suspension showed no significant cytotoxic effects. These findings suggest that SNEDDS may enhance the anticancer activity of andrographolide more effectively than polymeric micelles [12]. However, the relatively large droplet size (~145 nm) of the preliminary SNEDDS formulation suggests that further optimization is required to fully exploit the potential of this delivery system.

In parallel, understanding the molecular basis underlying the anticancer activity of andrographolide is essential. In renal cell carcinoma (RCC), vascular endothelial growth factor (VEGF) plays a central role in angiogenesis, which supports tumor growth and progression. Under VHL/HIF dysregulation, VEGF is upregulated and acts through tyrosine kinase receptors such as VEGFR. Besides its well-established role in endothelial cells, VEGF signaling has also been reported to occur in tumor cells, where it can activate major downstream pathways including PI3K/AKT/mTOR and RAS/RAF/MEK/ERK, thereby promoting tumor cell survival, proliferation, and migration. Given the clinical relevance of the VEGF/VEGFR axis in RCC, VEGFR-targeting tyrosine kinase inhibitors – such as sorafenib, sunitinib, and axitinib – have been approved and widely used in RCC treatment. Accordingly, this study employed molecular docking to investigate the potential binding interactions of andrographolide with VEGFR1 and VEGFR2, using axitinib as a reference inhibitor [13].

The formulation of SNEDDS based solely on a conventional trial-and-error strategy is both time-intensive and economically inefficient. This method relies on repeatedly combining excipients at various ratios and subsequently evaluating the resulting formulations according to selected performance parameters. The quality-by-design (QbD) concept, promoted by the United States Food and Drug Administration (US FDA), emphasizes a structured and knowledge-driven approach to pharmaceutical development. This strategy focuses on achieving consistent product quality by understanding and controlling the influence of formulation components and process parameters on critical quality attributes. To support this objective, experimental design methodologies are commonly applied to assess both individual and combined factor effects. Accordingly, a central composite design was employed in this work

owing to its efficiency in handling multiple variables and its suitability for modeling nonlinear relationships.

Based on this context, the study aimed to apply a design of experiments (DoE) approach to optimize an andrographolide-loaded SNEDDS and to investigate its potential mechanism in renal cell carcinoma through molecular docking targeting VEGFR1 and VEGFR2.

2. Materials and Method

2.1. Materials

ADG was supplied by AKScientific (India). Labrafil M 1944 CS and Transcutol HP were obtained from Gattefossé (France). Tween 80 was obtained from Singapore. Water was purified by reverse osmosis and then filtered in-house. All other reagents were analytical grade commercial products.

2.2. Methods

2.2.1. Preformulation Assessment of Andrographolide Raw Material

2.2.1.1. Solubility Study of Andrographolide

The solubility of andrographolide (ADG) in the raw *Andrographis paniculata* extract was determined in different media, including purified water, HCl pH 1.2, and phosphate buffers at pH 6.8 and 7.4, as follows: Approximately 0.1 g of the dried extract was added into centrifuge tubes containing 5 mL of the respective medium. The tubes were tightly sealed and placed in a shaking water bath at 120 rpm and 37°C for 48 hours. After equilibration, the samples were centrifuged at 5000 rpm for 20 minutes. The supernatant was carefully collected, filtered through a 0.2 µm regenerated cellulose membrane filter, and appropriately diluted with HPLC-grade methanol. The concentration of ADG in each sample was quantified using a validated high-performance liquid chromatography (HPLC) method. HPLC system (Shimadzu, Japan) consisted of UV detection with a C18 column (5 µm, 250 x 4.6 mm). The mobile phase was composed of methanol-water (55:45) at a flow rate of 1.0 mL/min, and the injection volume was 20 µl. The detection wavelength was set at 225 nm to determine the concentration of ADG.

2.2.1.2. Dissolution Study of Andrographolide

The dissolution profile of andrographolide (ADG) in the *Andrographis paniculata* extract was evaluated using the paddle apparatus (Erweka, Germany, Model DT60). An accurately weighed sample equivalent to approximately 30 mg of ADG was introduced into 900 mL of HCl pH 1.2, maintained at 37.0 ± 0.5°C and stirred at 100 rpm. At predetermined time intervals (5, 10, 15, 30, 45, and 60 minutes), 5 mL of the dissolution medium was withdrawn and initially filtered through filter paper (with the first portion discarded), followed by filtration through a 0.2 µm regenerated cellulose membrane filter. After each sampling, an equal volume of fresh medium pre-equilibrated at 37°C was added to maintain constant volume. The concentration of ADG at each time point was determined using high-performance liquid chromatography (HPLC).

2.2.1.3. Docking Studies

The chemical structures of andrographolide and axitinib (positive control) were built in MOE (version 2015.10) [14]. Their 3D geometries were then optimized using the force field AMBER99 and the partial charges were assigned using AM1-BCC. The crystal structures of VEGFR1 and VEGFR2 were obtained from the Protein Data Bank (PDB IDs: 3HNG and 1Y6A, respectively) [15]. For protein preparation, water molecules were removed and hydrogen atoms were added by protonation. Binding-site residues were energy-minimized in MOE using AMBER99 with the truncated Newton method. To validate the docking protocol, the co-crystallized ligand was removed and redocked into the active site; the protocol was considered valid when the redocked pose reproduced the native conformation with an RMSD < 2.0 Å. Using the same validated protocol, axitinib and andrographolide were docked into the active sites. For each receptor,

the top-ranked axitinib pose was used as a reference to guide the selection of the corresponding andrographolide pose. Docking scores were calculated using the London dG scoring function (E_score1, kcal/mol) and rescored using GBVI/WSA (E_score2, kcal/mol). All docking poses and interactions were visualized in Discovery Studio (version 2025 Client) [16].

2.2.1.4. In Silico Permeability Prediction

The Parallel Artificial Membrane Permeability Assay (PAMPA) of andrographolide was estimated using the ADMETlab 3.0 web server [17]. The canonical SMILES of andrographolide was submitted and the PAMPA output ($logP_{eff}$) was recorded under default settings. This permeability endpoint was used only to support the formulation rationale; other ADMET endpoints were not evaluated.

2.2.2. Preparation of SNEDDS Containing Andrographolide

Based on preliminary experiments, Labrafil M 1944 CS was used as the oil phase, Tween 80 was used as the surfactant, and Transcutol HP was used as the cosurfactant. Accurately weigh a specific amount of surfactant and cosurfactant into a glass vial, then add the oil phase and homogenize the mixture. Dissolve ADG in the mixture of oil, surfactant, and cosurfactant using a homogenizer until completely dissolved to obtain the andrographolide-loaded self-nanoemulsifying system. The system will be stored at room temperature until use.

2.2.3. Design of Experiments of SNEDDS

The design of experiments in formulation settings of SNEDDS was developed using Central Composite Face (CCF) design. The ratio of Labrafil M 1944 CS in the formulation and the ratio of Tween 80 in S_{mix} were chosen as independent variables. To eliminate any possible errors, all conditions relating to the preparation process were kept constant. As shown in Table 1, the screening ranges of the ratio of Labrafil M 1944 CS in the formulation and the ratio of Tween 80 in S_{mix} were 0.1-0.3 and 0.25-0.75, respectively. The dependent variables included droplet size and PDI of oil phase after addition of distilled water into SNEDDS and dissolution efficiency of ADG after 45 minutes (DE_{45}) in the Response Surface Methodology (RSM) model. The optimization criteria for the SNEDDS were to minimize droplet size and PDI while maximizing DE_{45}.

Table 1. Variables for Central Composite Face Design for Optimization of SNEDDS

Independent variables	Levels of factors			Dependent variables
	-1	0	1	
X_1: ratio of Labrafil M 1944 CS in the formulation	0.1	0.2	0.3	Y_1: Droplet size (nm)
X_2: ratio of Tween 80 in S_{mix}	0.25	0.5	0.75	Y_2: PDI
				Y_3: DE_{45} (%)

2.2.4. Emulsion Droplet Size Measurement

Samples were gently diluted 50 times with ultra-purified water, and measurements were taken at 25°C. Droplet size distribution of the microemulsion was studied using photon correlation spectroscopy (PCS) using a Malvern Zetasizer (Malvern Instruments, UK, Model Zetasizer Nano ZS90).

2.2.5. Thermodynamic Stability Studies

Thermodynamic stability was evaluated using heating-cooling cycles. The formulations were subjected to three consecutive heating–cooling cycles between 4 °C and 45 °C, with storage at each temperature for 24 hours. Afterward, each formulation was diluted with double-distilled water at a ratio of 1:50, and the

resulting nanoemulsions were examined for any signs of instability. Droplet size was subsequently measured to assess the effect of the temperature cycles on emulsion stability.

2.2.6. Dissolution Study

To compare the dissolution efficiency of different formulations, each SNEDDS formulation containing 40 mg of ADG was added to 900 mL of dissolution medium (phosphate buffer, pH 6.8) maintained at 37 ± 0.5°C and stirred at 100 rpm using the paddle apparatus (Erweka, Germany, Model DT60). At predetermined time intervals of 5, 15, 30, and 45 minutes, 5 mL of the dissolution medium was withdrawn and immediately replaced with an equal volume of fresh pH 6.8 buffer to maintain sink conditions. The collected samples were first filtered through a coarse filter and then through a 0.22 µm membrane filter (Sartorius, Germany, Model Minisart RC 25). The concentration of ADG in the filtrate was determined using a validated HPLC method. The dissolution efficiency (DE) of each formulation was calculated using the following equation:

$$DE = \frac{\int_{t_1}^{t_2} y.dt}{y_{100}.(t_2 - t_1)} \times (100)$$

Where y is the percentage of dissolved product; D.E. is the area under the dissolution curve between time points t_1, and t_2 expresses the percentage of the curve at maximum dissolution, y_{100}, over the same period.

3. Results and Discussions

3.1. Preformulation Assessment of Andrographolide

3.1.1. Solubility Study of Andrographolide

The solubility of Andrographolide (ADG) in the *Andrographis paniculata* extract in different media is presented in Table 2.

The results indicate that the solubility of ADG in purified water, HCl pH 1.2, and phosphate buffers at pH 6.8 and 7.4 is comparable. This observation is consistent with the structural characteristics of ADG, as it does not contain functional groups with sufficiently strong acidic or basic properties to undergo ionization in aqueous media.

Table 2. Solubility of ADG in the Andrographis paniculata extract

Medium	Solubility of ADG (µg/mL)
HCl pH 1.2	207.0 ± 3.0
Phosphate buffer pH 6.8	196.6 ± 9.1
Phosphate buffer pH 7.4	208.9 ± 2.2
Purified water	224.6 ± 7.8

3.1.2. Dissolution Study Of Andrographolide

The dissolution profile of ADG in the Andrographis paniculata extract in pH 1.2 medium is presented in Figure 1.

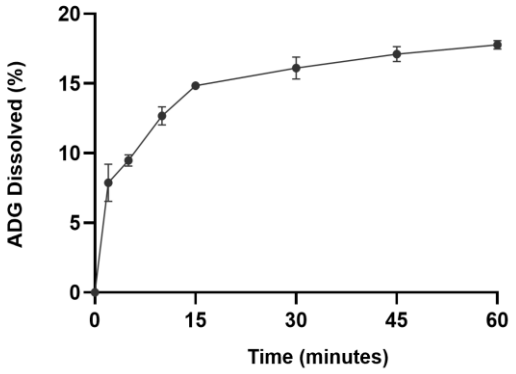

Figure 1. Dissolution profile of ADG in the raw extract (n = 3, mean ± SD).

The dissolution of ADG from the raw material is relatively low, with only 17.77 ± 0.30% released after 60 minutes. The slow dissolution rate and low solubility of ADG are among the factors that may adversely affect its absorption.

These findings demonstrate that a major limitation of andrographolide lies in its poor solubility and dissolution, which may compromise its therapeutic efficacy. Therefore, the development of appropriate drug delivery systems is essential to enhance its stability,

improve solubility, and potentially increase its permeability and targeted delivery to cancer cells.

Based on this rationale, the present study aims to optimize a self-nanoemulsifying drug delivery system (SNEDDS) containing andrographolide to overcome these limitations and optimize its therapeutic potential.

3.1.3. In silico Studies

To validate the docking protocol, the co-crystallized ligand in each protein was removed and redocked into the active site. The redocking results indicated that the selected protocol could reproduce the native binding pose and key interactions in 3HNG and 1Y6A, with RMSD values of 0.2917 Å and 1.0390 Å, respectively (Figure 2). The same validated procedure was then used to dock axitinib and andrographolide into the binding sites. The docking scores are reported in Table 3, and representative poses are shown in Figure 3.

Overall, the docking scores of andrographolide in the active sites of both targets were comparable to those of axitinib. In 3HNG, andrographolide and axitinib shared a similar interaction pattern, including hydrogen bonds with Glu878, His1020, and Asp1040, as well as hydrophobic contacts with Ile881, Leu882, and Leu1013. In 1Y6A, both ligands formed hydrophobic interactions with Leu838, Val846, Ala864, Val914, Cys917, Leu1033, and Phe1045. Notably, andrographolide also formed additional hydrogen bonds with Gly920 and Asn921 in 1Y6A, which may contribute to a more stable binding pose (Figure 3). These interactions are based on the top-ranked poses under the selected scoring scheme.

Docking suggested that andrographolide can adopt favorable binding poses within VEGFR1/VEGFR2, supporting its potential to modulate VEGF-related signaling. However, the predicted PAMPA permeability indicated limited passive membrane diffusion ($logP_{eff}$ = 0.916), which falls into the low-permeability range in ADMETlab ($logP_{eff}$ < 2.0). This low predicted permeability may contribute to reduced cellular exposure and supports the rationale for developing SNEDDS formulation to enhance membrane permeation.

Table 3. Docking scores (kcal/mol) of axitinib and andrographolide against VEGFR1 (3HNG) and VEGFR2 (1Y6A)

Ligand	Docking scores (kcal/mol)	
	3HNG	1Y6A
Axitinib	-8.5684	-6.4932
Andrographolide	-7.7329	-6.4383

(A): 3HNG (B): 1Y6A

Figure 2. Overlay of the native co-crystallized ligand (cyan) and the redocked pose (red) in (A) VEGFR1 (3HNG) and (B) VEGFR2 (1Y6A).

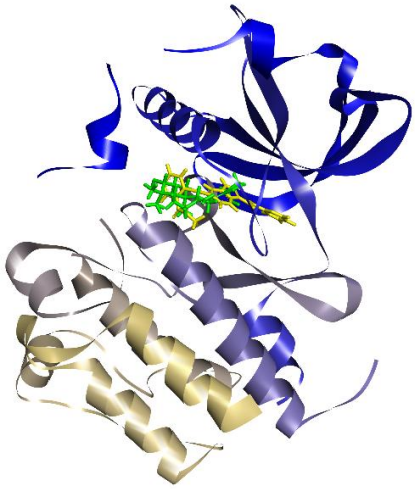

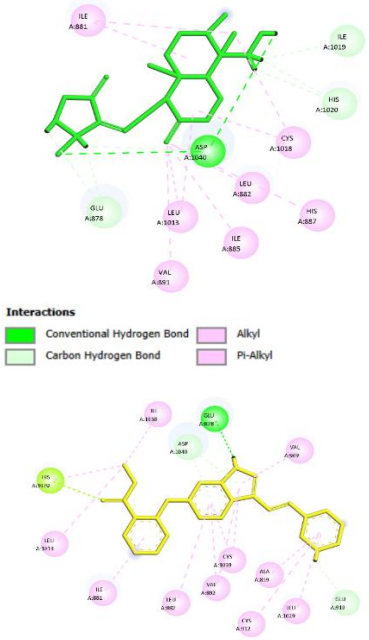

(A): 3HNG

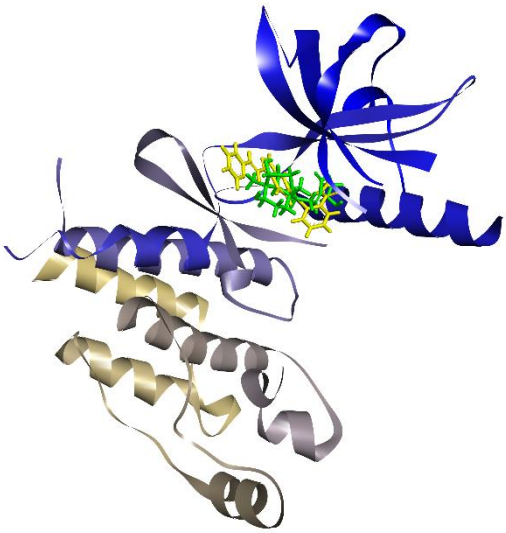

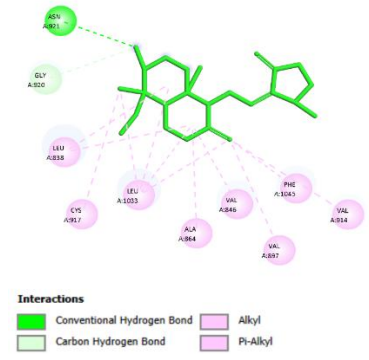

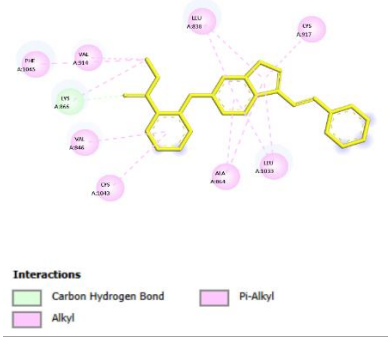

(B): 1Y6A

Figure 3. 3D docking poses (left) and 2D interaction diagrams (right) of axitinib (yellow) and andrographolide (green) in (A) VEGFR1 (3HNG) and (B) VEGFR2 (1Y6A).

Overall, the docking scores of andrographolide in the active sites of both targets were comparable to those of axitinib. In 3HNG, andrographolide and axitinib shared a similar interaction pattern, including hydrogen bonds with Glu878, His1020, and Asp1040, as well as hydrophobic contacts with Ile881, Leu882, and Leu1013. In 1Y6A, both ligands formed hydrophobic interactions with Leu838, Val846, Ala864, Val914, Cys917, Leu1033, and Phe1045. Notably, andrographolide also formed additional hydrogen bonds with Gly920 and Asn921 in 1Y6A, which may contribute to a more stable binding pose (Figure 3). These interactions are based on the top-ranked poses under the selected scoring scheme.

Docking suggested that andrographolide can adopt favorable binding poses within VEGFR1/VEGFR2, supporting its potential to modulate VEGF-related signaling. However, the predicted PAMPA permeability indicated limited passive membrane diffusion ($logP_{eff}$ = 0.916), which falls into the low-permeability range in ADMETlab ($logP_{eff}$ < 2.0). This low predicted permeability may contribute to reduced cellular exposure and supports the rationale for developing SNEDDS formulation to enhance membrane permeation.

3.2. Design of Experiments of SNEDDS

By using JMP Pro 18.0 software, eleven SNEDDS formulations constructed. The values of dependent variables were listed in Table 4.

Table 4. Design of experiment to evaluate the impact of oil and S_{mix} to SNEDDS

No	Independent variables		Dependent variables		
	X_1: ratio of Labrafil M 1944 CS in the formulation[a]	X_2: ratio of Tween 80 in S_{mix}[b]	Y_1: Droplet size (nm)	Y_2: PDI	Y_3: DE_{45} (%)
1	-1	1	11.90	0.151	64.49
2	-1	0	15.12	0.106	62.11
3	0	1	23.43	0.540	43.56
4	1	0	182.6	0.274	58.61
5	0	0	167.4	0.479	72.61
6	0	0	171.9	0.353	73.69
7	1	1	108.3	0.603	71.96
8	0	0	126.5	0.547	73.22
9	-1	-1	213.8	0.255	69.90
10	0	-1	290.5	0.229	66.98
11	1	-1	388.6	0.055	70.93
[a]X_1 [−1 (0.1), 0 (0.2), +1 (0.3)]. [b]X_2 [−1 (0.25), 0 (0.5), +1 (0.75)].					

3.2.1. Effect of single input variables (ratio of Labrafil M 1944 CS in the formulation and the ratio of Tween 80 in S_{mix}) and the interaction of these input variables on droplet size

Droplet size is one of the key characteristics to consider when developing a SNEDDS formulation, as it influences both the *in vitro* properties (such as solubility and stability) and the *in vivo* behavior of the system (such as drug absorption) solubility and permeability of the drug [20]. Generating a dispersion with small droplet size after dilution of SNEDDS with water or after lipid digestion is crucial, since such systems have been shown to minimize variations in oral dosage [21, 22].

In cancer therapy, droplet size is a critical parameter used for the passive targeting of therapeutic agents to tumor tissues [23]. The vascular system of tumors differs significantly from that of normal tissues: tumor blood vessels are larger, irregularly distributed, have a higher density, and exhibit greater permeability and leakiness [24]. This enhanced permeability and the leaky structure of tumor vasculature allow macromolecular drugs to accumulate within the tumor. This phenomenon, known as the enhanced permeability and retention (EPR) effect, enables nanosized drug delivery systems with droplet sizes smaller than approximately 150 nm to escape from the circulation through tumor capillaries, thereby increasing the concentration of chemotherapeutic drugs at the tumor site. Therefore, optimizing the droplet size of SNEDDS is essential.

Table 5. Impact of oil and S_{mix} to Droplet size and PDI of SNEDDS

Regression coefficient	Droplet size (nm)		PDI	
	Value	p	Value	p
Constant	281.93	0.0005	-0.0547	0.0002
	1693.2596	0.0034	5.0442	0.1030
X_1	-1044.343	0.0003	-0.8710	0.0159
X_2	-784	0.3043	6.52	0.0128
X_1*X_2	1425.316	0.5371	-19.0105	0.0170
X_1*X_1	701.62947	0.0972	0.0703	0.9384
X_2*X_2	281.93	0.0005	-0.0547	0.0002

The construction of a quadratic regression equation describing the effect of input variables on droplet size (EQ_1) showed that the model was statistically significant (p regression = 0.0019 < 0.05) and fitted well with the experimental data, consistent with the prediction results of the CCF model (R^2 = 0.96 > 0.8). From Table 5, the obtained regression equation (EQ_1) is expressed as:

$$Y_1 = 281.93 + 1693.2596X_1 – 1044.343X_2$$

The regression equation indicates that droplet size is mainly influenced by two input variables: the proportion of oil (O) in the formulation and the proportion of surfactant (S) in the S_{mix}. The positive coefficient of O (1693.2596) suggests a synergistic effect of oil content on droplet size. As the oil content increases, droplet size increases, and vice versa. The contour plot (Figure 4) also illustrates the synergistic influence of oil proportion on droplet size. Experimentally, this was confirmed through formulations F9, F10, and F11, where increasing the oil content led to larger droplet sizes (213.8 nm, 290.5 nm, and 388.6 nm, respectively). This can be explained by the increase in interfacial tension between the oil and aqueous phases when the oil content rises, while the amount of surfactant is insufficient to completely cover all the oil droplets and reduce interfacial tension, increasing droplet size [25].

Meanwhile, increasing the surfactant concentration led to a reduction in droplet size. Specifically, formulations with higher S proportions in S_{mix}, such as F1 and F2, showed smaller droplet sizes (11.90 and 15.12 nm, respectively), consistent with the negative regression coefficient of X_2 (–1044.343), as illustrated by the contour plots in Figure 4. This result confirms that the surfactant plays a crucial role in reducing droplet size, as Tween 80 accumulates at the oil–water interface, helping to decrease interfacial tension between the two phases and forming a mechanical barrier that prevents droplet coalescence [26].

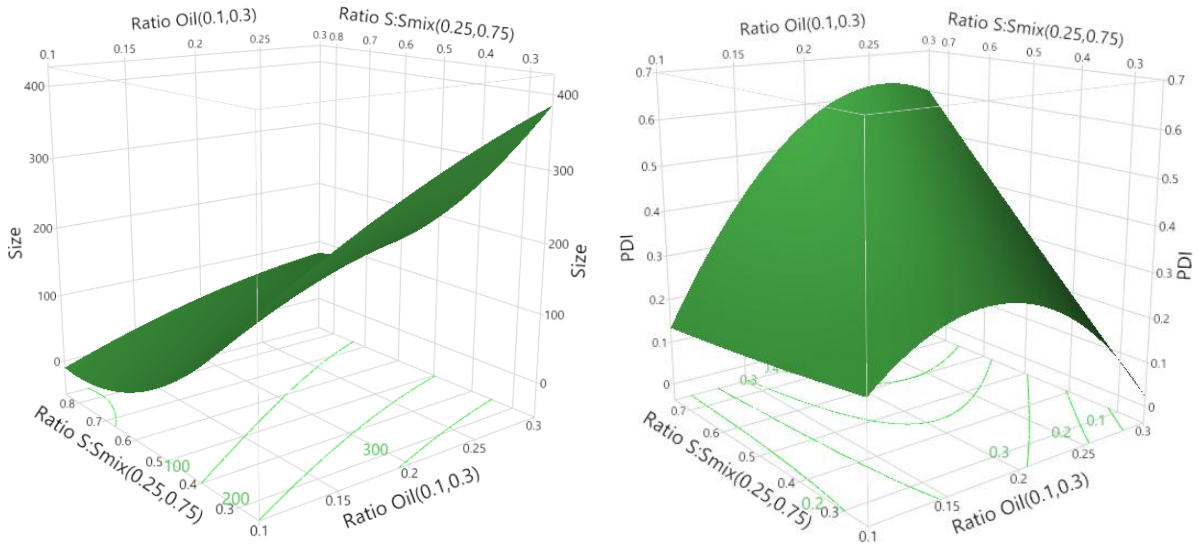

(a) (b)

Figure 4. Respone surface plots illustrating the effects of the independent variables on the dependent variables (Y_1) and (Y_2).

3.2.2. Effect of Single Input Variables (Ratio of Labrafil M 1944 CS in the Formulation and the Ratio of Tween 80 in S_{mix}) and the Interaction of these Input Variables on PDI

The effect of input variables on the particle size distribution (PDI) was also evaluated. The quadratic regression equation describing the influence of input variables on PDI (EQ_2) showed statistical significance ($p = 0.0159 < 0.05$) and a good fit between experimental and predicted results ($R^2 = 0.90 > 0.8$). From Table 5, it can be seen that the regression coefficients of X_2, X_1X_2, X_1X_1, and the constant term have $p < 0.05$, indicating statistical significance. Therefore, the regression equation for the output variable (Y_2) is expressed as:

$$Y_2 = -0.0547 - 0.8710X_2 + 6.52X_1X_2 - 19.0105X_1X_1$$

From the regression equation of Y_2, it can be observed that three main factors influence PDI: the proportion of surfactant in S_{mix} (X_2), the interaction between X_1 and X_2, and the quadratic effect of the oil proportion in the formulation (X_1), making it difficult to separately analyze the effect of each individual factor. Therefore, using contour plots is more feasible for comprehensively analyzing the combined influence of all factors.

As shown in the contour plot of Y_2 (Figure 4), when both the oil proportion in the formulation and the surfactant proportion in S_{mix} increase simultaneously, the PDI also increases. Notably, an increase in oil content led to a significant rise in PDI, as evidenced experimentally by formulations F1, F3, and F7. When the oil proportion in the formulation increased from 0.1 to 0.3 while the surfactant proportion in S_{mix} remained constant (0.75), the corresponding PDI values increased from 0.151 to 0.540 and 0.603, respectively. However, when the oil proportion was kept low (0.1–0.15), Figure 4 shows that increasing the amount of surfactant did not markedly change the PDI, which remained at a low level (0.1–0.2). This was further confirmed in formulations F1 and F2, which exhibited PDI values of 0.151 and 0.106, respectively.

From this analysis, it can be observed that the surfactant and co-surfactant, Tween 80 and Transcutol HP, had limited effects on reducing PDI in this self-nanoemulsifying system. In

contrast, increasing the oil content led to higher polydispersity of droplet size, as the increased oil amount raises the interfacial free energy, rendering the system thermodynamically less stable. Consequently, the emulsion droplets tend to coalesce, resulting in a broader droplet size distribution.

3.2.3. Effect of Single Input Variables (Ratio of Labrafil M 1944 CS in the Formulation and the Ratio of Tween 80 in S_{mix}) and the Interaction of these Input Variables on DE_{45}

For dissolution efficiency (DE_{45}, %), the mathematical equation (EQ_3) showed no statistical significance with $p = 0.9018 > 0.05$, and did not fit the experimental results well, as indicated by the very low values of $R^2 = 0.22$ and adjusted $R^2 = -0.5546$. This could be explained by one or both of the following reasons: (1) the investigated ranges of oil and S_{mix} concentrations were relatively narrow (0.1–0.3) and therefore did not adequately reflect their actual roles, and/or (2) the drug release evaluation method was not entirely suitable for the SNEDDS system.

The study adopted the conventional dissolution method using a USP II apparatus under sink conditions. The results showed that all formulations rapidly dispersed to form nanoemulsions and reached saturated concentration within 15 minutes, making it difficult to distinguish between their dissolution profiles. Moreover, the conventional dissolution test is not truly specific for differentiating and screening lipid-based drug delivery systems, as *in vivo*, the physical and chemical properties of the formulation change significantly after oral administration due to interactions with bile and pancreatic fluids, similar to lipid digestion from food, which in turn alters the release behavior of the system. Therefore, to gain a better understanding of the release characteristics and overall performance of the formulation, a more specific model than the conventional dissolution test should be employed, such as an *in vitro* lipolysis model, which can simulate and predict the fate of the drug released from the SNEDDS within the gastrointestinal tract.

3.2.4. Optimization of SNEDDS Formulation

Table 6. Optimized SNEDDS formulation

Dependent variables	Predicted values	Experimental values
Y_1: Droplet size (nm)	12	12.02 ± 0.2483
Y_2: PDI	0.152	0.113 ± 0.017

After establishing the relationships between the dependent variables and the independent variables, the optimal formulation was determined using JMP Pro 18 software based on the desirability function. The individual desirability functions for the dependent variables, denoted as H_1 and H_2, correspond to particle size and PDI, respectively. Optimization was not performed for the $DE_{0\text{-}45}$ variable because the second-order regression model for $DE_{0\text{-}45}$ did not adequately describe the effects of the two independent variables. The overall desirability function was defined as follows: assuming that all dependent variables have equal importance (importance = 1), the overall desirability function to obtain the optimal formulation is given by: $H = H_1^{1/2}. H_2^{1/2}$. After the optimization process, the optimal values of the independent variables were determined as an oil ratio in the formulation (X_1) = 0,1 and a surfactant ratio in S_{mix} (X_2) = 0,61. The predicted values of the dependent variables are presented in Table 6.

3.2.5. Stability Studies

The main difference between an emulsion and a nanoemulsion lies in their thermodynamic stability. SNEDDS form nanoemulsions through *in situ solubilization*, and such systems must maintain stability to prevent precipitation, creaming, or phase separation (cracking). However, in many cases, prolonged storage can lead to drug precipitation from the system; crystal nuclei may appear and grow into larger crystals, which then settle at the bottom, thereby affecting drug absorption and therapeutic efficacy [7].

Therefore, to evaluate the thermodynamic stability of the system, heating-cooling cycles were performed, and none of the 11 formulations showed any signs of phase separation or drug crystallization. Based on the results shown in Table 7, it can be generally observed that the formulations exhibited droplet size changes after dilution within an acceptable range, with variations not exceeding 2–3 times the initial values and PDI mostly remaining below 0.4 (except for formulations F7 and F8), indicating uniform and stable dispersions. Formulations F1–F3 showed a slight or negligible increase in droplet size, while formulations F10–F11 exhibited a slight decrease in droplet size but still maintained relatively higher values compared to other formulations. In practice, formulations F1–F2 demonstrated high stability and had compositions close to that of the optimized formulation.

Table 7. Droplet size (nm) and polydispersity index (PDI) of ADG SNEDDS formulations after dilution with distilled water following heating-cooking cycles (n = 3, mean ± SD)

No	Before hearing-cooling cycles		After heating-cooling cycles	
	Droplet size (nm)	PDI	Droplet size (nm)	PDI
F1	11.90 ± 0.06	0.151 ± 0.012	17.32 ± 2.01	0.296 ± 0.038
F2	15.12 ± 0.04	0.106 ± 0.009	15.50 ± 0.36	0.143 ± 0.029
F3	23.43 ± 0.49	0.540 ± 0.049	22.12 ± 0.36	0.375 ± 0.019
F4	182.6 ± 0.9	0.274 ± 0.007	311.4 ± 12.56	0.233 ± 0.032
F5	167.4 ± 1.3	0.479 ± 0.028	246.3 ± 3.68	0.252 ± 0.005
F6	171.9 ± 0.8	0.353 ± 0.008	252.7 ± 3.45	0.253 ± 0.008
F7	108.3 ± 8.7	0.603 ± 0.018	73.11 ± 2.25	0.642 ± 0.029
F8	126.5 ± 0.7	0.547 ± 0.006	116.0 ± 2.33	0.636 ± 0.024
F9	213.8 ± 3.6	0.255 ± 0.025	194.5 ± 5.02	0.241 ± 0.004
F10	290.5 ± 13.5	0.229 ± 0.019	252.2 ± 4.45	0.302 ± 0.007
F11	388.6 ± 15.9	0.055 ± 0.014	351.3 ± 15.32	0.198 ± 0.009

4. Conclusion

In the present study, a self-nanoemulsifying drug delivery system (SNEDDS) for andrographolide was successfully optimized using a design of experiments (DoE) approach. Preformulation studies demonstrated that andrographolide exhibits poor solubility and limited dissolution, which may compromise its pharmaceutical performance. Following optimization, the optimal formulation was obtained at an oil fraction of 0.10 and a surfactant fraction in S_{mix} of 0.61. The optimized SNEDDS exhibited a mean droplet size of 12.02 ± 0.25 nm, a PDI of 0.113 ± 0.017, and good thermodynamic stability after heating-cooling cycles. The SNEDDS formulation significantly improved the dissolution behavior of andrographolide compared to the raw material, indicating its potential to overcome dissolution-limited performance. In parallel, molecular docking studies indicated that andrographolide is capable of forming favorable interactions within the active sites of VEGFR1 and VEGFR2, providing preliminary insight into a potential molecular mechanism relevant to RCC. Furthermore, the low predicted passive permeability supports the rationale for employing a lipid-based delivery system to overcome the biopharmaceutical limitations of andrographolide. Collectively, these findings demonstrate that DoE-guided optimization of a SNEDDS, supported by preformulation insights, represents a rational and effective strategy to enhance the dissolution and overall pharmaceutical performance of andrographolide.

Acknowledgments

This research is funded by Vietnam National Foundation for Science and Technology Development (NAFOSTED) under grant number NCUD.03-2023.03.

Conflicts of Interest

The authors report there are no competing interest to declare.

References

[1] I. Khan, S. Mahfooz, M. Faisal, A. A. Alatar, I. A. Ansari, Andrographolide Induces Apoptosis and Cell Cycle Arrest through Inhibition of Aberrant Hedgehog Signaling Pathway in Colon Cancer Cells, Nutritional Cancer, Vol. 73, No. 11-12, 2021, pp. 2428-2446, https://doi.org/10.1080/01635581.2020.1828942.

[2] X. R. Wang, Z. B. Jiang, C. Xu, W. Y. Meng, P. Liu, Y. Z. Zhang et al., Andrographolide Suppresses Non-small-cell Lung Cancer Progression through Induction of Autophagy and Antitumor Immune Response, Pharmacological Research, Vol. 179, 2022, Article 106198, doi: https://doi.org/10.1016/j.phrs.2022.106198.

[3] J. Li, L. Huang, Z. He, M. Chen, Y. Ding, Y. Yao, et al., Andrographolide Suppresses the Growth and Metastasis of Luminal-like Breast Cancer by Inhibiting the NF-κB/miR-21-5p/PDCD4 Signaling Pathway, Frontiers in Cell and Developmental Biology, Vol. 9, 2021, Article 643525, https://doi.org/10.3389/fcell.2021.643525.

[4] Y. C. Lee, H. H. Lin, C. H. Hsu, C. J. Wang, T. A. Chiang, J. H. Chen, Inhibitory Effects of Andrographolide on Migration and Invasion in Human Non-small Cell Lung Cancer A549 Cells via Down-regulation of PI3K/Akt Signaling Pathway, European Journal of Pharmacology, Vol. 632, No. 1, 2010, pp. 23-32, https://doi.org/10.1016/j.ejphar.2010.01.009.

[5] Z. Malik, R. Parveen, B. Parveen, S. Zahiruddin, M. A. Khan, A. Khan et al., Anticancer Potential of Andrographolide from Andrographis paniculata (Burm.f.) Nees and its Mechanisms of Action, Journal of Ethnopharmacology, Vol. 272, 2021, Article 113936, https://doi.org/10.1016/j.jep.2021.113936.

[6] L. Ye, T. Wang, L. Tang, W. Liu, Z. Yang, J. Zhou et al., Poor Oral Bioavailability of a Promising Anticancer Agent Andrographolide is Due to Extensive Metabolism and Efflux by P-glycoprotein, Journal of Pharmaceutical Sciences, Vol. 100, No. 11, 2011, pp. 5007-5017, https://doi.org/10.1002/jps.22693.

[7] N. Parmar, N. Singla, S. Amin, K. Kohli, Study of Cosurfactant Effect on Nanoemulsifying Area and Development of Lercanidipine Loaded Self-nanoemulsifying Drug Delivery System, Colloids and Surfaces B: Biointerfaces, Vol. 86, No. 2, 2011, pp. 327-338, https://doi.org/10.1016/j.colsurfb.2011.04.016.

[8] D. Cun, C. Zhang, H. Bera, M. Yang, Particle Engineering Principles and Technologies for Pharmaceutical Biologics, Advanced Drug Delivery Reviews, Vol. 174, 2021, pp. 140-167, https://doi.org/10.1016/j.addr.2021.04.006.

[9] M. Abdulkarim, P. K. Sharma, M. Gumbleton, Self-emulsifying Drug Delivery System: Mucus Permeation and Innovative Quantification Technologies, Advanced Drug Delivery Reviews, Vol. 142, 2019, pp. 62-74, https://doi.org/10.1016/j.addr.2019.04.001.

[10] D. E. Large, R. G. Abdelmessih, E. A. Fink, D. T. Auguste. Liposome Composition in Drug Delivery Design, Synthesis, Characterization, and Clinical Application, Advanced Drug Delivery Reviews, Vol. 176, 2021, Article 113851, https://doi.org/10.1016/j.addr.2021.113851.

[11] S. S. Timur, R. N. Gürsoy. Design and In vitro Evaluation of Solid SEDDS for Breast Cancer Therapy, Journal of Drug Delivery Science and Technology, Vol. 60, 2020, Article 102023, https://doi.org/10.1016/j.jddst.2020.102023.

[12] N. T. Nguyen, N. Q. Do, T. M. P. Nguyen, C. K. Cao, T. T. H. Duong, N. T. Tung, Formulation and In vitro Cytotoxicity Evaluation of Andrographolide-loaded Nano Delivery Systems in the Renca Renal Cancer Cell Line, Pharmaceutical Sciences Asia, Vol. 53, No. 1, 2026, pp. 78-91, https://doi.org/10.29090/psa.2026.01.25.4856.

[13] L. Xiong, Y. Zhang, J. Wang, M. Yu, L. Huang, Y. Hou et al., Novel Small Molecule Inhibitors Targeting Renal Cell Carcinoma: Status, Challenges, Future Directions, European Journal of Medicinal Chemistry, Vol. 267, 2024, Article 116158, https://doi.org/10.1016/j.ejmech.2024.116158.

[14] Chemical Computing Group, Research Citing MOE, https://www.chemcomp.com/en/Research-Citing_MOE.htm (accessed on: January 6th, 2026).

[15] RCSB Protein Data Bank, Homepage, https://www.rcsb.org/ (accessed on: January 6th, 2026).

[16] BIOVIA Discovery Studio, Dassault Systèmes, https://www.3ds.com/products/biovia/discovery-studio (accessed on: January 6th, 2026).

[17] ADMETlab 3.0, https://admetlab3.scbdd.com/server/evaluationCal (accessed on: January 6th, 2026).

[18] T. Yi, J. Wan, H. Xu, X. Yang, A New Solid Self-microemulsifying Formulation Prepared by Spray-drying to Improve the Oral Bioavailability of Poorly Water Soluble Drugs, European Journal of Pharmaceutics and Biopharmaceutics, Vol. 70, No. 2, 2008, pp. 439-444, https://doi.org/10.1016/j.ejpb.2008.05.001.

[19] M. M. Kamal, S. Nazzal. Novel Sulforaphane-enabled Self-microemulsifying Delivery Systems of Taxanes: Formulation Development and In vitro Cytotoxicity Against Breast Cancer Cells, International Journal of Pharmaceutics, Vol. 536, No. 1, 2018, pp. 187-198, https://doi.org/10.1016/j.ijpharm.2017.11.063.

[20] J. X. Zhu, D. Tang, L. Feng, Z. G. Zheng, R. S. Wang, A. G. Wu et al., Development of Self-microemulsifying Drug Delivery System for Oral Bioavailability Enhancement of Berberine Hydrochloride, Drug Development and Industrial Pharmacy, Vol. 39, No. 3, 2013, pp. 499-506, https://doi.org/10.3109/03639045.2012.683875.

[21] J. M. Kovarik, E. A. Mueller, J. B. van Bree, W. Tetzloff, K. Kutz. Reduced Inter- and Intraindividual Variability in Cyclosporine Pharmacokinetics from a Microemulsion Formulation, Journal of Pharmaceutical Sciences, Vol. 83, No. 3, 1994, pp. 444-446, https://doi.org/10.1002/jps.2600830336.

[22] F. S. Nielsen, K. B. Petersen, A. Müllertz. Bioavailability of Probucol from Lipid and Surfactant Based Formulations in Minipigs: Influence of Droplet Size and Dietary State, European Journal of Pharmaceutics and Biopharmaceutics, Vol. 69, No. 2, 2008, pp. 553-562, https://doi.org/10.1016/j.ejpb.2007.12.020.

[23] M. R. Mozafari, A. Pardakhty, S. Azarmi, J. A. Jazayeri, A. Nokhodchi, A. Omri, Role of Nanocarrier Systems in Cancer Nanotherapy, Journal of Liposome Research, Vol. 19, No. 4, 2009, pp. 310-321, https://doi.org/10.1080/08982100902913204.

[24] P. Y. Aw Yong, P. Gan, A. Sasmita, S. T. Mak, A. Ling, Nanoparticles as Carriers of Phytochemicals: Recent Applications Against Lung Cancer, International Journal of Research in Biomedical and Biotechnology, Vol. 7, 2018, pp. 1-11, https://doi.org/10.1080/17425247.2022.2041599.

[25] Y. Tian, Y. Guo, W. Zhang, Effect of Oil Type, Aliphatic Alcohol, and Ionic Surfactants on the Formation and Stability of Ceramide-2 Enriched Nanoemulsions, Journal of Dispersion Science and Technology, Vol. 37, No. 8, 2016, pp. 1115-1122, https://doi.org/10.1080/01932691.2015.1083440.

[26] H. Reiss. Entropy-induced Dispersion of Bulk Liquids, Journal of Colloid and Interface Science, Vol. 53, No. 1, 1975, pp. 61-70.